BTRA SCAN VOL. LII NO. 4 OCT. 2023

Study of structural and optical properties of aluminium-doped ZnO films on polyethylene terephthalate substrate via radio-frequency sputtering

Abhishek Panwar[1]**, Nishant Chandel**[2]**, Sanjay Kumar**[3]*****

[1]Department of Polymer and Process Engineering (DPPE), Indian Institute of Technology Roorkee, Saharanpur Campus, Saharanpur, Uttar Pradesh, India 247001

[2]Carbon fibre lab, The Bombay Textile Research Association, Ghatkopar, Mumbai, India 400086

[3]Department of Physics, J.V. Jain College, Saharanpur, Uttar Pradesh, India 247001

Abstract

Al/ZnO films, which are ZnO doped with aluminium, were created by radio-frequency magnetron sputtering in this instance. Polyethylene terephthalate was used as a substrate to prepare Al/ZnO films. The radio frequency (RF) magnetron sputtering power varied from 120 to 140W. Through the use of ultraviolet (UV), field emission scanning electron microscopy (FE-SEM), and X-ray diffraction (XRD), this article investigates the effects of varying the radio frequency power during magnetron sputtering while film production is underway. The XRD confirmed the (002) and (102) planes specific to the hexagonal wurtzite structure. We also found that the average crystallite size decreased from 25.56 to 24.11 nm with the change of RF power in the deposition. In addition, the energy band gap shrank from 3.58 to 3.56 eV. As spherical grains become visible, SEM images show that the surface morphology of the produced films has changed preferentially. The refractive index, film surface roughness, and energy band gap decreased as the RF magnetron sputtering power increased.

Key words:

Composites, Thin Films, Magnetron Sputtering, Flexible electronics, Wearable electronics

Citation

Abhishek Panwar, Nishant Chandel, Sanjay Kumar - “Study of structural and optical properties of aluminium-doped ZnO films on polyethylene terephthalate substrate via radio-frequency sputtering”, *BTRA Scan* - Vol. LII No. 4, Oct. 2023, Page no. 13 to 15

1.0 Introduction

Zinc oxide is known as a potential candidate for transparent conductive oxide (TCO) due to its direct energy band-gap in the range of 3-3.37 eV and significant excitonic binding energy of 60 meV. It also has quite impressive and distinctive structural and optical properties.[1,2] It is a n-type semiconductor having a wurtzite crystal structure. It is thermally and chemically stable, less expensive, abundantly available, and non-toxic [3,4]. Therefore, the preparation of ZnO thin films for various applications such as chemical and bio-sensors [5], catalysts [6], UV photodetectors [7], Schottky diodes8, and light-emitting diodes9 is currently in use. It is transparent to visible light and can be made highly conductive by doping. The TCO that is now in use is indium tin oxide (ITO); however, it is not a good option because it is poisonous, brittle, expensive, and less stable for H_2 plasma [10]. TCO film's excellent transparency and conductive qualities have led to their widespread use as flexible electrical devices [11]. TCO is frequently employed in piezoelectric transducers, solar cells, photodetectors, and light-emitting diodes because it produces excellent electrical conductivity when doped with aluminium. However, most of the aforementioned devices are made with Silicon wafers as substrates limiting their potential application of flexible electronics. In this work, we studied the structural, morphological, and optical properties of Al/ZO thin films on polyethylene terephthalate (PET) substrate. Here, we used 2.5% Al-doping by weight of ZnO. The film's thickness significantly impacts the deposited thin films, which are highly crystalline and aligned. We will investigate the structural, morphological, optical, and electrical aspects of the Al/ZnO films deposited using RF magnetron sputtering powers.

2.0 Experimental procedure

Al/ZnO thin films (unit model: 12 "MSPT) were deposited on an ITO-coated PET substrate using RF magnetron sputtering). ZnO: Al (2.5 wt. % Al_2O_3) was used as the target material for the deposition of film. The substrates were

---

*Corresponding author,
E-mail: physicistinnano@gmail.com

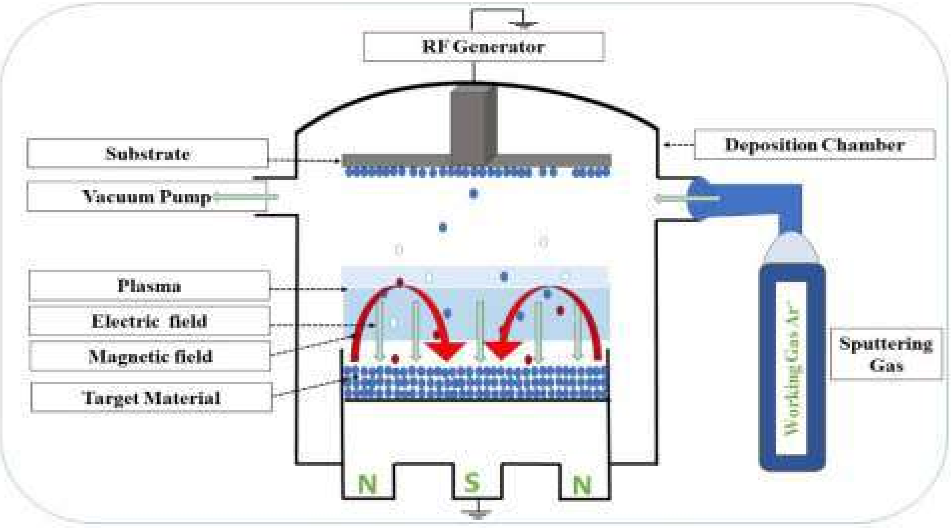

Figure 1. Schematic setup of RF Magnetron Sputtering

ultrasonically cleaned in acetone and deionized water for 10 minutes before thin film deposition. Sputtering gas, or argon, was added into the vacuum chamber after it had been evacuated and pushed down to 4.0×10^{-6} Torr. The thin film deposition technique involved maintaining a pressure of 3.0×10^{-2} Torr throughout and using two radio frequency magnetron sputtering powers, 120 W and 140 W for 20 minutes.

2.1 X-ray Diffraction Pattern (XRD)

Fig. 2 shows the XRD spectrum for Al/ZnO thin films deposited by the RF magnetron sputtering method on PET as substrates with different power, 120W and 140W. ZnO thin film patterns exhibited diffraction planes at (002) and (102) corresponding to the hexagonal wurtzite structure of Zinc oxide, and other diffraction patterns at (222) and (113) represented the mixed phase of aluminium oxide and aluminium oxide (indicated by * and by $ respectively) [11,12]. A broader PET substrate pattern, indicated by #, was also acquired. Equation 1, where d is the interplanar spacing for the plane (hkl), and hkl are miller indices, was used to compute the lattice parameters 'c' given in Table 1 from (002) peaks,

$$\frac{1}{d^2} = \frac{4}{3a^2}(h^2 + hk + k^2) + \frac{l^2}{c^2} \quad \text{..................(1)}$$

The Debye Scherrer formula was applied to find the crystallite size,

$$D = \frac{0.9\,\lambda}{\beta\,\cos\theta} \quad \text{..................(2)}$$

Where λ is the X-ray wavelength (1.54 Å), θ is Bragg's diffraction angle, and β is the full-width half-maximum of (002) peak of the XRD pattern [13]. It was observed that there was no independent peak for aluminium doping in the ZnO thin films. It is since there is a difference in ionic radii of Zn^{2}+(0.74Å) and Al^{3}+(0.54Å). Because of the small ionic radii of aluminium, it gets induced in the interstices of the ZnO structure without altering the wurtzite structure of ZnO [14].

Table 1. Showing the various parameters of Al/ZnO films

Sample	Position [2θ]	FWHM	Lattice Parameter (c) Å	Crystallite size (nm)	Optical bandgap. (Eg) (eV)
120 W	34.43	0.323	5.220	25.56	3.56
140 W	34.33	0.345	5.203	24.11	3.58

The tabular data observation indicates that as the RF magnetron sputtering power increases, the crystallite size and the band gap decrease, showing that aluminium is being absorbed into interstices suitably.

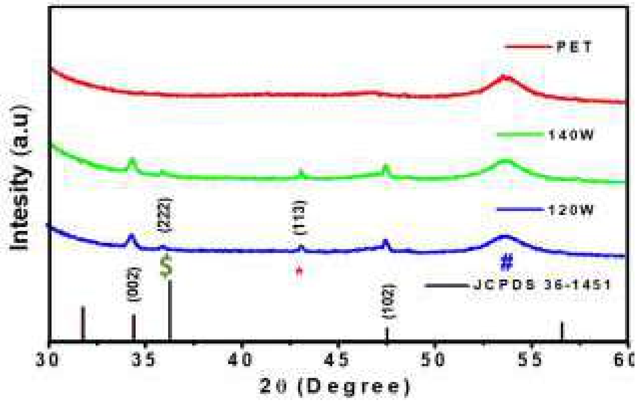

Fig. 2 XRD Spectrum of the Al/ZnO thin films at different Radio Frequency magnetron sputtering powers.

2.2 Field Emission Scanning electron microscopy (FE-SEM)

The surface morphology of Al/ZnO thin films on PET substrate was analyzed by FE-SEM as shown in fig 3(a) & (b). Both films showed signs of spherical grain growth. Surface roughness and Grain size were increased rapidly with the increasing sputtering power from 120W to 140W [15,16]. Spherical grains were uniformly distributed on the substrate, confirming the good adhesion to the substrate. It also considers that grain growth occurs because of the annealing of the thin film, which results in a significant driving force for internal atomic diffusion for grain growth.

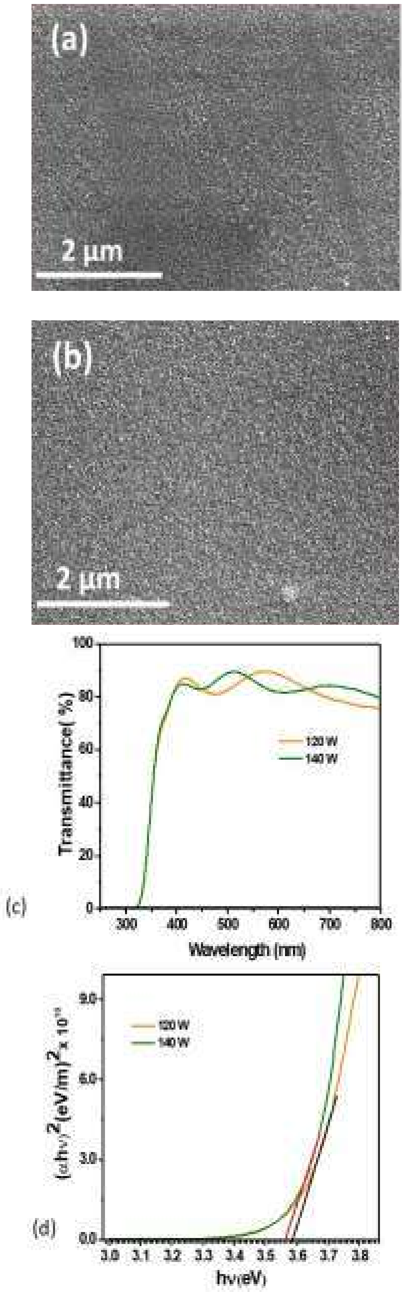

Fig. 3SEM imagesat (a) 120W; (b) 140W.(c) Optical transmittance as a function of wavelength (d)Tauc's plot for the optical energy band gap of the Al/ZnO thin films at various substrate RF magnetron sputtering powers.

2.3 Optical Study

Fig. 3(c) & (d) displays the optical transmittance of the Al/ZnO thin films deposited at various RF magnetron sputtering powers. The transmittance spectra of Al/ZnO thin films were measured between 250 and 800 nm in wavelength. It was observed that both the thin-film samples showed 80% average transmittance in the visible wavelength range. [17]

The optical energy band gap of Al/ZnO thin films was calculated using $(\alpha h\upsilon)^2$ versus hυ plots, which resulted in a straight-line fit to the absorption edge of the glass and extrapolation to the $(\alpha h\upsilon)^2 = 0$ axis. It gives a way to produce an optical energy band gap. As for allowed direct transition, the variation of $(\alpha h\upsilon)^2$ with photon energy obeys Tauc's plot method.

$$(\alpha h\upsilon)^2 = A(h\upsilon - E_g) \quad \text{..........................} (3)$$

Where A is the equation constant, Eg is the optical band gap, h is Planck's constant, and α is the absorption coefficient. The value for optical band gaps for both films is given in Table 1. The Eg values were found to be 3.58 and 3.56eV for 120 W and 140 W, respectively. The energy band gap was found to be inversely proportional to the power of Radio Frequency magnetron sputtering. It decreases the carrier concentration, moderating the wide optical band gap [17].

3.0 Conclusion:

This study successfully deposited Al/ZnO thin films on ITO-coated PET substrates with Radio Frequency magnetron sputtering. Hexagonal wurtzite structure with (002) and (102) orientation for ZnO structure was confirmed from XRD patterns. The morphological studies showed that the growth of spherical grains in Al/ZnO thin films was more uniform with the increasing power of Radio Frequency magnetron sputtering in film deposition. The decrease in energy band gap and crystalline size of Al/ZnO films with the increasing of substrate Radio Frequency magnetron sputtering power indicate that control of deposition power is an excellent tool to change the properties of Al/ZnO films. Varying the Radio Frequency magnetron sputtering power of the substrate during film deposition makes the materials developed in this study suitable for use in solar cells, TCO, and flexible/wearable electronics.

References

1. Özgür Ü, Alivov YI, Liu C, et al. A comprehensive review of ZnO materials and devices. J Appl Phys. 2005;98(4):1-103. doi:10.1063/1.1992666
2. Pellegrino D, Franzò G, Strano V, Mirabella S, Bruno E. Improved synthesis of ZnO nanowalls: Effects of chemical bath deposition time and annealing temperature. Chemosensors. 2019;7(2):1-10. doi:10.3390/chemosensors7020018
3. Li XY, Li HJ, Wang ZJ, et al. Effect of substrate temperature on the structural and optical properties of ZnO and Al-doped ZnO thin films prepared by dc magnetron sputtering. Opt Commun. 2009;282(2):247-252. doi:10.1016/J.OPTCOM.2008.10.003
4. Kim IH, Ku DY, Ko JH, et al. Improvement of the thermal and chemical stability of Al doped ZnO films. J Electroceramics. 2006;17(2-4):241-245. doi:10.1007/s10832-006-8315-8
5. Ahmad R, Tripathy N, Hahn YB. Wide linear-range detecting high sensitivity cholesterol biosensors based on aspect-ratio controlled ZnO nanorods grown on silver electrodes. Sensors Actuators B Chem. 2012;169:382-386. doi:10.1016/J.SNB.2012.05.027
6. Upadhyay GK, Rajput JK, Pathak TK, Kumar V, Purohit LP. Synthesis of ZnO: TiO2 nanocomposites for photocatalyst application in visible light. Vacuum. 2019;160:154-163. doi:10.1016/J.VACUUM.2018.11.026
7. Young SJ, Liu YH. High Response of Ultraviolet Photodetector Based on Al-Doped ZnO Nanosheet Structures. IEEE J Sel Top Quantum Electron. 2017;23(5):1-5. doi:10.1109/JSTQE.2017.2684540
8. Chaitra U, Muhammed Ali A V., Mahesha MG, Kompa A, Kekuda D, Mohan Rao K. Property evaluation of spin-coated Al doped ZnO thin films and Au/AZO/FTO Schottky diodes. Superlattices Microstruct. 2021;155(November 2020):106903. doi:10.1016/j.spmi.2021.106903
9. Sun Y, Wang W, Zhang H, et al. High-Performance Quantum Dot Light-Emitting Diodes Based on Al-Doped ZnO Nanoparticles Electron Transport Layer. ACS Appl Mater Interfaces. 2018;10(22):18902-18909. doi:10.1021/acsami.8b04754
10. Liu H, Avrutin V, Izyumskaya N, Özgr Ü, Morkoç H. Transparent conducting oxides for electrode applications in light emitting and absorbing devices. Superlattices Microstruct. 2010;48(5):458-484. doi:10.1016/j.spmi.2010.08.011
11. Farhat OF, Halim MM, Abdullah MJ, Ali MKM, Ahmed NM, Bououdina M. Fabrication and characterization of ZnO nanowires by wet oxidation of Zn thin film deposited on Teflon substrate. Superlattices Microstruct. 2015;86:236-242. doi:10.1016/j.spmi.2015.07.056
12. Faraj MG, Ibrahim K. Optical and structural properties of thermally evaporated zinc oxide thin films on polyethylene terephthalate substrates. Int J Polym Sci. 2011;2011. doi:10.1155/2011/302843
13. Wang W, Ai T, Yu Q. Electrical and photocatalytic properties of boron-doped ZnO nanostructure grown on PET-ITO flexible substrates by hydrothermal method. Sci Rep. 2017;7(January):1-11. doi:10.1038/srep42615
14. Chouikh F, Beggah Y, Aida MS. Physical Properties of Undoped and Doped ZnO Thin Films Prepared by Spray Pyrolysis for Photovoltaic Application. Int J Thin Film Sci Technol. 2014;3(2):51-56. doi:10.12785/ijtfst/030204
15. Sauki NS adah M, Muhamad NA, Zahid FS, Herman SH, Rizman ZI. The structural and electrical properties of nanostructures ZnO thin films on flexible substrate. Int J Adv Sci Eng Inf Technol. 2017;7(3):822-828. doi:10.18517/ijaseit.7.3.986
16. Liu H, Lei C. Low-temperature deposited Titanium-doped zinc oxide thin films on the flexible PET substrate by DC magnetron sputtering. Vacuum. 2011;86(4):483-486. doi:10.1016/j.vacuum.2011.10.006
17. Şenay V. Some physical properties of nanostructured Al doped ZnO thin films synthesized by RF magnetron sputtering at room temperature. J Mater Sci Mater Electron. 2019;30(10):9910-9915. doi:10.1007/s10854-019-01329-6

BTRA Facility :

DSC : Differential scanning calorimeter (DSC) is a method of thermal analysis that determines the temperature and heat flow associated with material transitions as a function of temperature or time.

Some of the important application of DSC are

1) Glass Transition
2) Melting Point
3) % Crystallinity
4) Specific Heat
5) Curing Kinetics
6) Oxidative Induction Time (OIT)

We have DSC 8000 with high pressure assembly in which we can go upto maximum 500psi. It is very useful for studying high pressure Oxidation Induction Time (HPOIT) of oils, Polyolefin Geosynthetics etc. under pressure.

Contact for more details :
Email : info@btrainida.com
Tel. : +91-22-6202 3636